

DEDICATED INSTRUMENTATION FOR HIGH SENSITIVITY, LOW FREQUENCY NOISE MEASUREMENT SYSTEMS

C. CIOFI, G. GIUSI and G. SCANDURRA

Dipartimento di Fisica della Materia e TFA and INFN, Salita Sperone, 31 I-98166, Messina, Italy

B. NERI

Dipartimento di Ingegneria dell'Informazione, Via Diotisalvi, 2 I-56100, Pisa, Italy

Received 8 August 2003

Accepted 21 March 2004

Low Frequency Noise Measurements (LFNM) can be used as very sensitive tool for the characterization of the quality and the reliability of electron devices. However, especially in those cases in which the frequency range of interest extends below 1 Hz, instrumentation with an acceptable low level of background noise is not easily found on the market. In fact, at very low frequencies, the flicker noise introduced by the electronic components which make up the instrumentation becomes predominant and several interesting phenomena which could be detected by means of LFNM may result completely hidden in the background noise. This consideration is not limited to the case of input preamplifiers but does extend to any piece of instrumentation that contributes to the LFNM systems, and in particular to the power supplies used for biasing the Device Under Test. During the last few years, our research groups have been strongly involved in the design of very low noise instrumentation for application in the field of LFNM. In this work we report the main results which we have obtained together with a discussion of the design guidelines that have allowed us, in a few cases, to reach noise levels not to be equalled by any instrumentation available on the market.

Keywords: Noise measurements; spectral analysis; low noise instrumentation; electron device.

1. Introduction

Since the late 1960s, Low Frequency Noise Measurement (LFNM) technique has been used as a tool for the analysis of conduction mechanisms in solid state devices and for the characterization of the quality of electron devices[1]. The analysis of the Low Frequency Noise (LFN) has become more and more important with time as we have moved towards the present VLSI era and it is bound to become even more important as we approach device dimensions in the nanometric range. In fact, the increasing miniaturization leads to a significant increase in the noise to signal ratio, thus making noise one of the main limiting factors for pursuing the ultimate miniaturization limits. Moreover, as LFN can be used as a probe capable of investigating the phenomena occurring at a microscopic scale, it can be useful for characterizing the quality and the reliability of microelectronic materials and devices. The most important peculiarities of LFNM technique with respect to

this specific application field can be summarized as follows: (a) it is not destructive; (b) it is highly sensitive to localized phenomena; (c) it does not require complicated procedures for the preparation of the samples and expensive instrumentation.

Therefore the LFNM technique can be advantageously used for a not invasive and not expensive reliability analysis of many failure mechanisms occurring in electron devices. Several evidences of the capability of LFNM to serve as a tool for the characterization of the reliability of electron devices are reported in the literature since '70 [2,3] and a comprehensive review of the application of LFNM to the characterization of different failure mechanisms can be found in [4] and in the references therein.

Unfortunately, notwithstanding the potential advantages of LFNMs based characterization techniques, their use is not yet as widespread as they would deserve. Sensible noise measurements, especially at very low frequencies ($f < 1\text{Hz}$), are not easily performed as several spurious effects often superimpose to the noise signal to be detected. Besides the external interferences which could be, at least in principle, completely removed by proper electrical, mechanical and thermal shielding, the instrumentation itself may become the limiting factor because it contributes with its own internal noise to set the minimum level of detectable signal. At very low frequencies, thermal noise does not usually play an important role. It is the flicker noise ($1/f$ noise), particularly the one introduced by the active devices used in electronic instrumentation, which plays the most important role. Commercial instrumentation, with rare exceptions, is characterized by a quite high level of flicker noise thus considerably limiting the field of application of LFNMs technique.

The feeling of our research groups, founded on more than 15 years of experience in the field, is that a skill in the design and realization of low noise instrumentation can represent a key factor for obtaining the full advantages out of the application of LFNM technique to the characterisation of electron devices and materials. The main purpose of this paper is to provide the reader with a review of the several issues connected with the realization of specific instrumentation for LFNMs and with a discussion of the solutions which we have adopted for solving several specific problems.

2. Dedicated Instrumentation for LFNM

A simplified block diagram of the several pieces of instrumentation which make up almost any conceivable LFNM system is reported in Fig. 1.

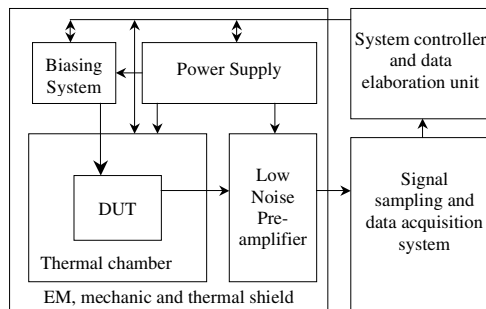


Fig.1. Block diagram of an automated LFNM system.

It refers to the ideal and desirable case in which all the measurement parameters, especially the temperature of the thermal chamber and the bias of the DUT can be set by means of an external controller, usually a Personal Computer (PC), in order to make automated noise measurements possible. However, this is seldom the case, especially because although a few examples of low noise programmable biasing sources have been demonstrated [5,6], their use is still limited either because of their size and high cost, or because of the complication involved in their integration as a standard piece of instrumentation in LFNM systems. In the following subsections we will address a few issues relative to each specific component of a LFNM system.

2.1. Input preamplifiers

By means of a careful design, the Equivalent Input Voltage Noise (EIVN) of a voltage amplifier can be reduced to that of the active device used in the first stage of the amplifying chain. In order to avoid disturbances coming from the power supply and other common mode interferences (temperature fluctuations, EM interferences and so on) the use of differential configurations is mandatory. As the best performances in terms of EIVN are to be found in discrete devices, we usually resort to discrete components input stages. We have selected the matched BJT pair SSM2220 by PMI as the devices with the lowest EIVN (1.5, 3, 10 nV/[Hz]^{1/2} at 1, 0.1, and 0.01 Hz, respectively). The performances of an ultra low noise amplifier based on the SSM2220 can be found in [7]. With such a design, we obtain the best performances in term of EIVN (curve labelled BJT in Fig. 3). However, when the equivalent impedance of the source is above a few tens of ohms, the effect of the Equivalent Input Current Noise (EICN) of the BJTs becomes predominant. In these cases a JFET input stage is preferable, although the best discrete devices we have been able to select (IF3601 discrete JFET by InterFet) have a significantly higher EIVN. In the case of the JFETs, however, the EICN is enormously lower thus making them the ideal choice for high impedance DUTs. Moreover, as the required biasing current is in the order of a few pA, AC coupling down to the mHz range is readily obtained. Figure 2 shows an example of a JFET input stage low noise preamplifier.

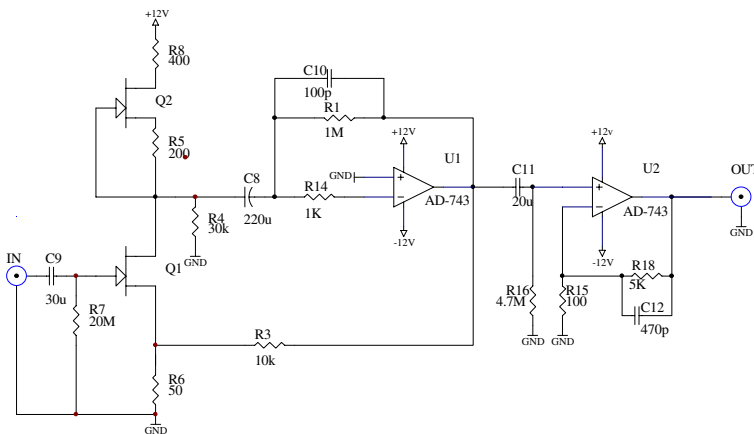


Fig. 2. Schematic of a JFET input stage ultra low noise preamplifier.

The first stage of the amplifier can be regarded as a cascade of a JFET transconductance amplifier coupled to a transresistance amplifier, which realize a two stage high gain

voltage amplifier in a shunt series feedback configuration with a gain of about 200 (set by the ratio $R3/R6$). The transistor Q2 acts as a current source for providing high gain and high PSSR notwithstanding that we do not use a differential configuration. The second stage, which is AC coupled to avoid saturation due to the output offset of the first stage, provides for an overall 80 dB voltage gain. The input and intermediate high pass filters provide for a low corner frequency of about 2 mHz.

When the performances of our amplifiers are compared to those of commercially available instrumentation, the improvement which can be obtained at very low frequencies is remarkable. As an example, the EIVN spectra of our BJT and JFET preamplifiers are compared to that of the popular Brookdeal 5003 in Fig. 3.

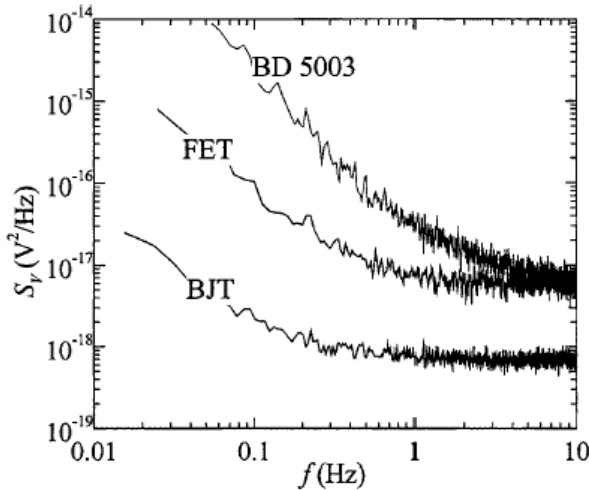


Fig. 3. Noise performances of different LN amplifiers.

In the case of transresistance amplifiers, the main contribution to the output noise often comes from the high value resistor which is used in a shunt parallel configuration for obtaining a high transresistance gain as in Fig. 4, where the equivalent input noise sources of the operational amplifier and the equivalent voltage noise source of the feedback resistor are shown. If the virtual short circuit approximation holds, the transresistance gain is equal to R_R and, in the case of DUT impedances much higher than the input impedance of the transresistance amplifier, the spectral density $S_{ineq}(f)$ of the equivalent input current noise source of the entire system can be estimated as follows:

$$S_{ineq}(f) = S_{in} + \frac{S_{vn}}{R_R^2} + \frac{4kT}{R_R} \tag{1}$$

In the case of a transresistance gain of 100 M Ω , the noise due to R_R (the third term in Eq. 1) amounts to about $166 \times 10^{-30} \text{ A}^2/\text{Hz}$. In order for the second term (noise due to the equivalent voltage input source of the operational amplifier) to be comparable with such a value, S_{vn} should be in the order of $1.6 \times 10^{-12} \text{ V}^2/\text{Hz}$ (that is $1.3 \text{ } \mu\text{V}/[\text{Hz}]^{1/2}$). This clearly demonstrates that for the realization of low noise transresistance amplifiers we must resort to operational amplifiers with a very low EICN, while quite high values of EIVN can be tolerated. In our recent designs we resort to the MOSFET input operational amplifier TLC070 which is characterized by an EICN as low as $3.6 \times 10^{-31} \text{ A}^2/\text{Hz}$ and by

and EIVN of about $90 \text{ nV}/[\text{Hz}]^{1/2}@1 \text{ Hz}$. Eq. 1 also shows that increasing R_R is beneficial as far as the equivalent input noise is concerned. However, there are limitations to the value that R_R can assume. In fact, it is sometimes difficult to AC couple the device under test to the input of the amplifier and therefore the DC component of the current must flow across R_R without saturating the operational amplifier. Moreover, the bandwidth of the amplifier is often limited by the parasitic capacitance in parallel to R_R . Since for a given resistor technology and package such a capacitance is almost independent of the resistance value, the bandwidth decreases proportionally to R_R . The observation that the BN of a transresistance amplifier is mostly due to the feedback resistor, has recently lead us to explore the possibility of designing transresistance amplifiers which use a noiseless impedance in the feedback loop rather than a resistance. This can be done by employing a feedback capacitor instead of the resistor R_R in Fig. 4. This idea has lead us to the design of a new topology for the realization of a high gain, low noise, high bandwidth transresistance amplifiers. The schematic of the new topology is reported in Fig. 5.

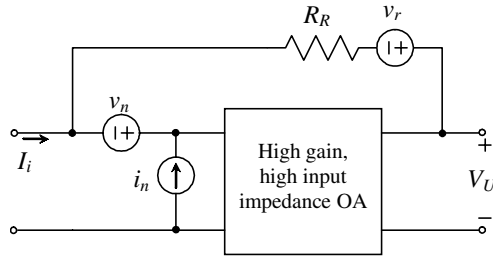


Fig. 4. Simplified schematic of a transresistance amplifier.

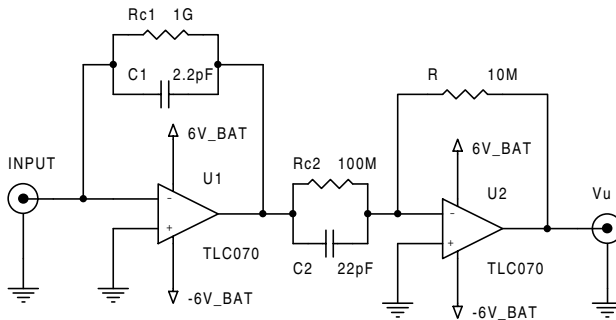


Fig. 5. New topology for a low noise, high bandwidth transresistance amplifier configuration.

The resistor R_{c1} provides for a DC feedback path for the first operational amplifier. The condition $R_{c1} \times C_1 = R_{c2} \times C_2$ must be satisfied in order to have a flat response down to DC. In the virtual short circuit approximation, the transresistance gain A_{R0} results:

$$A_{R0} = \frac{C_2}{C_1} R = 100 \text{ M}\Omega . \tag{2}$$

It can be demonstrated that the new approach allows, for the same transresistance gain, to obtain an increase of the bandwidth by a factor C_2/C_1 and a reduction of the EICN by the same factor[8]. This last advantage can be obtained in the case in which the resistance R_{C1} can be made large enough not to significantly contribute to the output noise. However, the larger R_{C1} , the lower is the DC input current that can be tolerated by the amplifier without causing the saturation of the first stage. A comparison between the performances which can be obtained by using the new approach with respect to the conventional one (for the same transresistance gain and using the very same operational amplifiers and resistance types) is given in Fig. 6.

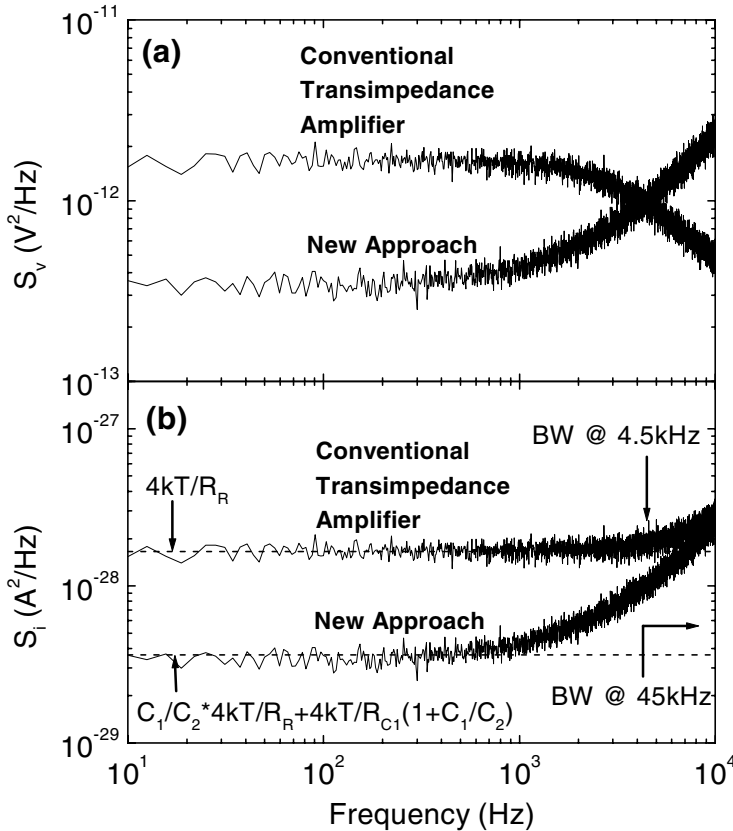


Fig. 6. Comparison of the noise performances between the new and the conventional transresistance amplifiers (open input). In (a), the power spectra of the voltage fluctuations at the output are reported. In (b) the spectra of the equivalent input current noise source corresponding to the curves in (a) are reported.

The increase of the output noise above 1 kHz is due to the combined effect of the EIVN and of the common mode parasitic input capacitance of the operational amplifier. The same effect is present in the conventional design, but it is hidden because of the limited bandwidth and the much higher level of white noise. This is clearly shown in Fig. 6b, where the calculated EICN power spectral densities are reported. If we compare our new design with commercial instrumentation (the popular SR570 by Stanford Research, and

two among the best amplifiers available on the market by FEMTO), we obtain better performances both when we compare the bandwidth for the same equivalent input noise and when we compare the equivalent input noise for the same bandwidth (Table 1).

Table 1. Comparison of the performances of different transresistance amplifiers.

Same equivalent input noise ($\approx 4 \times 10^{-29}$ A ² /Hz)			
	New design (4×10^{-29} A ² /Hz)	SR570 (2.5×10^{-29} A ² /Hz)	LCA-4K-1G (4.2×10^{-29} A ² /Hz)
Bandwidth:	45 kHz	10 Hz	4 kHz
Same bandwidth (≈ 45 kHz)			
	New design (45 kHz)	SR570 (20 kHz)	LCA-40K-100M (40 kHz)
Eq. Inp. Noise:	4×10^{-29} A ² /Hz	3.6×10^{-25} A ² /Hz	3.6×10^{-28} A ² /Hz

2.2. Bias sources

Solid state bias sources are normally useless in the case of LFNM because of the high level of $1/f$ noise produced by the zener which is used as a reference in all these systems. Therefore, batteries are normally used for providing voltage bias to the DUT. Current bias is usually obtained by connecting a few batteries in series and using a conveniently large series resistor. Batteries behave as low frequency noise voltage or current sources provided that they do not supply too much current. As a rule of thumb (for measurements down below 100 mHz) a battery should not supply a current higher than that needed to fully discharge it in less than 100 hours. In any case, the voltage or current supplied by a battery drops with time and therefore it is never the same in repeated measurements. Moreover, only a discrete set of voltages are available. One can resort to resistive voltage dividers, but in this case, for the system to behave as a low internal resistance voltage source, the current supplied by the battery must be quite large thus making the problem of the discharge more and more important. Remote control of the voltage value is not possible and therefore a lot of time is wasted in changing the configuration of the battery packs or for just monitoring its actual value. The problem of realizing reliable low noise voltage or current sources (either programmable or not) is never an easy one because the level of noise introduced by such devices directly appears at the ends of the DUT. In the course of the last few years we have addressed the problem of the realization of fixed and programmable bias sources and we believe that some of our results are remarkable and deserve to be mentioned here.

2.2.1. Fixed value low noise voltage and current sources

Almost any battery, when supplying a very low current, may behave as a very low noise, high stability voltage reference. In fact, while the exact value of the generated voltage does depend on the charge state of the batteries (for rechargeable batteries) or on their age (for non rechargeable ones), if the battery does not supply current, its value may be assumed almost constant. Accurate measurements performed in a highly stabilized temperature chamber (30 ± 0.005 °C) have shown that the voltage drop (mainly due to self discharge) is in the order of 100 ppm/h in the case of lead acid batteries (Sonnenschein Dryfit A300, 6.8 V, 1.1 Ah), while in the case of lithium batteries (Duracell type 223, 6 V) the voltage drift can be as low as 3 ppm/h.

Even in the case of the lead acid battery, the voltage drift results 14 mV in 24 hours which is largely acceptable for many applications. Therefore, in most applications we use

small capacity lead acid battery as references for low noise solid state voltage sources. A simple circuit which behaves as a low noise voltage source is illustrated in Fig. 7(a).

The high value resistor R in series with the battery is necessary in order to avoid that the battery discharges through the Gate-Source junction of the JFET when V_{DD} is turned off. The capacitor C is then required for filtering out the thermal noise generated by the resistor. With a careful design of the RC time constant, the power spectrum of the voltage fluctuations at the output of the system reduces to that introduced by the EIVN of the JFET. The resistance R_D is needed in order to maintain the drain-source voltage below the value for which impact ionization in the channel becomes significant. When employing the large area JFET IF3601 by Interfet, voltage noise as low as 5×10^{-15} , 10^{-16} , 10^{-17} V²/Hz at 0.01, 0.1 and 1 Hz, respectively, can be obtained.

Using a battery as a reference, we can also realize a low noise current source using the configuration reported in Fig. 7(b). Here the reference battery together with the source resistance R_S sets the current value according to the following equation:

$$I_{OUT} = \frac{V_B - V_{GS}}{R_S} \tag{3}$$

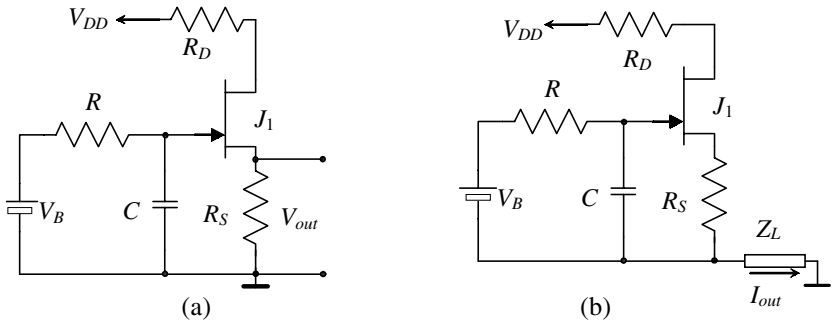


Fig. 7. Schematic of a LN fixed voltage source (a), and of a LN fixed current source (b).

Using values of V_B in the order of a few volts (for instance 6 V by employing a lead acid battery) one may neglect, as a first approximation, the value of V_{GS} which can be in the range of a few hundreds mV for the IF3601. By neglecting the contribution of the noise produced by the battery and by the resistance R (the thermal noise produced by the resistance R is filtered out by the capacitor C), the power spectral density of the current fluctuations delivered to the load can be estimated as follows:

$$S_{I_{out}} = (S_{enFET} + 4kTR_S) \times \left(\frac{g_m}{1 + g_m R_S} \right)^2 \tag{4}$$

where S_{enFET} is the power spectral density of the EIVN of the JFET and g_m is the transconductance of the JFET. When employing the large area JFET IF3601, values of g_m in the order of 200 mA/V are easily obtained. The actual circuit used for realizing a practical low noise current noise source is more complex with respect to the one shown in Fig. 7, because, as in the case of the voltage sources, we must avoid too large values of V_{DS} independently of the load impedance Z_L . The circuit we use is described in [9]. As an example of the performances which can be obtained, the power spectra at the output of

our current source are reported in Fig. 8 for different values of the current (I_G in the figure) supplied to a $200\ \Omega$ load. Such a current source has been successfully used to demonstrate the feasibility of low noise measurements at wafer level as described in [10].

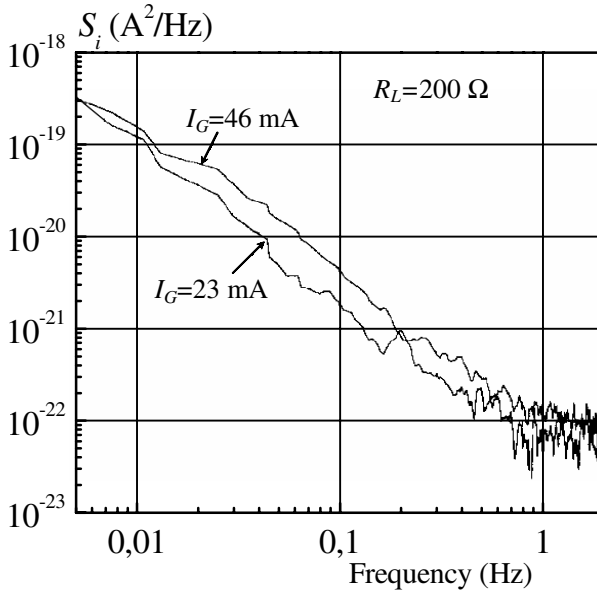


Fig. 8. Current noise at the output of an ultra low noise current source.

2.2.2. Programmable low noise voltage sources

Designing programmable low noise voltage or current sources is not an easy task since standard DA converters produce a high level of low frequency noise. Moreover, the digital circuitry needed for the operation of a programmable source is likely to introduce interferences which degrade the noise performances. Up to now we have however successfully addressed the issue of designing and realizing programmable, high accuracy, ultra low noise voltage sources. In one case, we used a low noise fixed value voltage source as a reference for a low noise resistive voltage divider ladder network. The output of such a ladder network was used as the input of a low noise power voltage follower to provide low output impedance and high current driving capability. Such a piece of instrumentation behaves as a very low noise 12 bit DA converter capable of generating voltages in the range from 0 to 8 V with an accuracy better than $\pm 1.5\ \text{mV}$ and delivering to the load currents in the range of a few hundred mA. Typical values of the spectral density of the voltage fluctuations at the output are 10^{-12} , 10^{-15} , $10^{-16}\ \text{V}^2/\text{Hz}$ at 0.01, 0.1 and 1 Hz, respectively [5].

In many applications, however, the ability to supply currents in the range of a few mA may be sufficient. This prompted us to verify the possibility of realizing a programmable low noise voltage reference by directly filtering the output noise of a standard solid state DA converter. With reference to Fig. 9(a), if the time constant of the RC filter in the figure is sufficiently high, the high level of noise produced by a standard solid state DA converter (more than 50 dB above that corresponding to the EIVN of the IF3601 in the

frequency range below 1 Hz) could be filtered out starting from a conveniently low frequency. However, it may be calculated that at $f=100$ mHz, in order to reduce the noise generated by a “low noise” commercial DA converter (in the order of 10^{-10} V²/Hz at 100 mHz) to a level at least 10 dB below that of the EIVN of the JFET (10^{-16} V²/Hz at 100 mHz), a time constant of about 30 minutes would be required, thus making the use of the device impractical because one would have to wait a few hours before having a stable output upon any change of the voltage to be generated. In order to overcome this limitation, we resorted to the circuit shown in Fig. 9(b) which is part of a microcontroller based control system as described in [6]. The optically controlled analog switch (H11F1) behaves as a very high resistance with the driving LED switched off ($R_{off}>300$ M Ω), while it behaves as a small value resistance when the LED is turned on. The LED may be automatically operated by the microcontroller, being switched ON in order to speed up the voltage change transient. When the new steady state condition is reached, the LED is switched off in such a way as to allow the low pass filter to develop its full action.

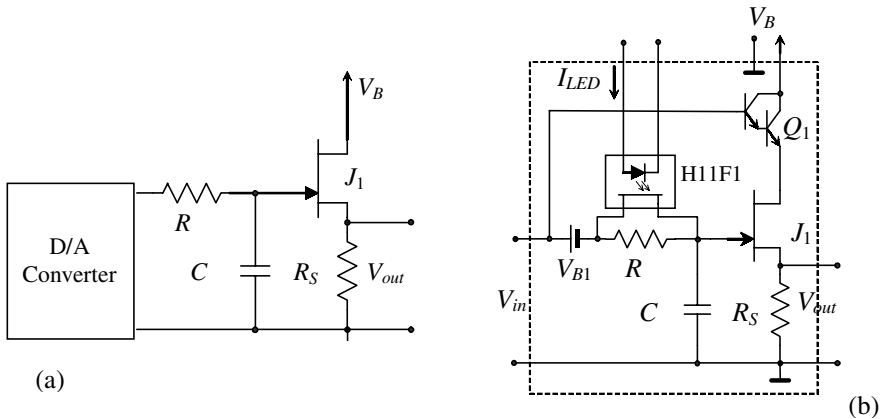


Fig. 9. A simple implementation of a low noise voltage reference (a); in (b) the actual implementation of the output stage, that allows to obtain reduced set-up times, is shown.

In fact, while the output voltage is changing, no noise measurement would be meaningful and by means of the procedure described above, the new steady state is reached in a matter of a few minutes. We decided to employ two high capacity 12 V, 6Ah lead acid batteries, one for the control board and one for the output buffer, in order to reduce the size of the entire system. For the output voltage to reach 0 V we had therefore to insert the battery V_{B1} which insures that the JFET is pinched off when the input voltage is close to 0 V. At the same time the battery allows, together with the darlington Q1, to maintain the JFET in saturation with the lowest possible value of V_{DS} . The battery V_{B1} , through which only the negligible gate current flows, is obtained as the series of 3 tiny 100 mAh NiCd cells. The voltage at the output of the circuit in Fig. 9(b) is continuously monitored by means of a high resolution AD converter and a digital control loop is used in order to drive the DA converter section for obtaining high accuracy and stability. Proper countermeasures were taken in order to reduce the interferences generated by the action of the control loop [6]. The noise performances which can be obtained are impressive as can be noted in Fig. 10, where, together with the power spectrum of the voltage fluctuations S_{out} measured at the output of the voltage source, we have reported the power spectrum at the

output of the solid state voltage source (REF192) which provides the reference for the DA converter used in the design. Accuracy and stability of the supplied voltage are within $\pm 250 \mu\text{V}$ in the entire output range from 0 to 5 V.

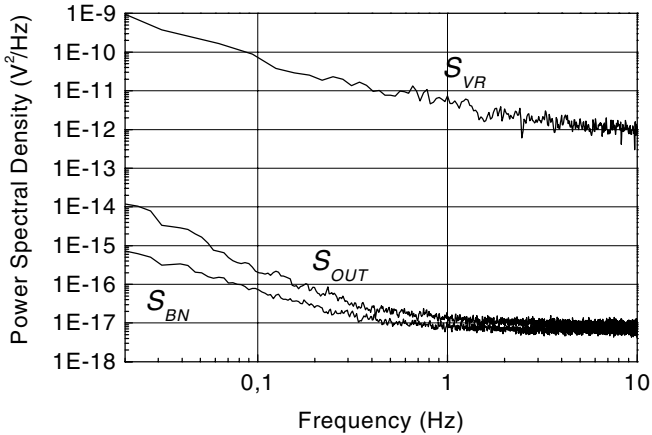


Fig. 10. Noise performances of the digitally programmable low noise voltage source. S_{BN} is the BN noise of the measurement system, S_{VR} is the noise of the voltage reference of the DA employed in the design.

2.3. Low noise thermal chamber

Often, LFNMs must be performed on samples maintained at a fixed temperature [11]. Standard thermal chambers for reliability tests cannot be used because of the high level of temperature fluctuations and insufficient shielding. In the past we have been using miniaturized heaters that were battery supplied in order to allow to put them in the shielded measurement environment. More recently, because of the need for a thermal chamber large enough for hosting several samples and with the capability of allowing long term noise measurements [12], we had to face the problem of the design of a high stability thermal chamber capable of meeting these requirements. In a thermostatic chamber, the residual thermal fluctuations are primarily due to the environmental perturbations and to the fluctuation of the power source which supplies the heaters. In the case of our design [13], the choice has been made to use a two stage thermal structure in which two coaxial aluminum vessels are separated by a thermal insulating layer (PTFE). This structure, shown in Fig. 11, acts as a second-order low-pass filter, effectively reducing the effects of environmental perturbations and heaters power fluctuations. This solution has allowed a reduction of more than 90 dB of the temperature fluctuations with respect to an oven chamber of equivalent dimensions and using the same mass of aluminum and the same external insulation structure. The sample chamber can reach a maximum temperature of 250°C with a stability better than 0.1°C . The effectiveness of the design was such that we were not able, using the best instrumentation we had available, to evaluate the residual thermal fluctuations within the sample chamber [13]. The internal heater directly in contact with the inner chamber (Fig. 11) is supplied only during start up in order to reduce the time required for reaching a steady state temperature in the sample chamber. The aluminum bottom cap, together with a metallic pipe running without any interruption through the outer insulation layer and across the entire shielded box into which the thermal

chamber lays, allows an effective insulation from the electromagnetic interferences originating from the cables which connect the heaters to the external solid state power supply.

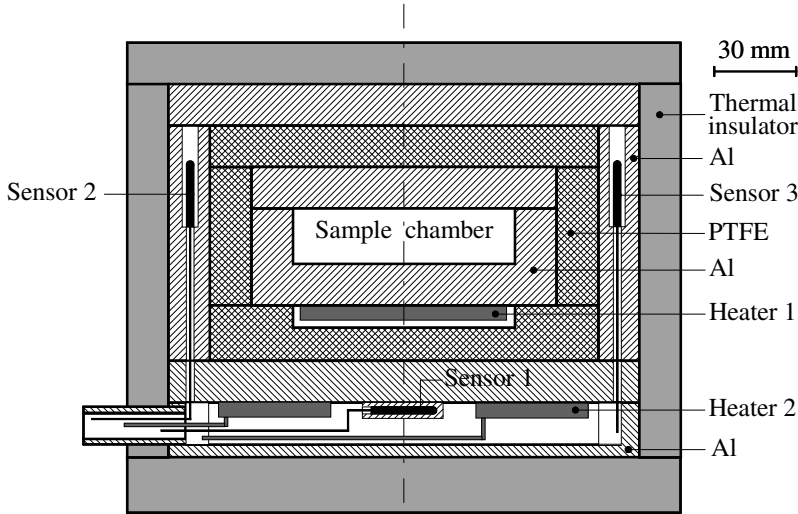


Fig.11. Double stage, low temperature noise thermal chamber for LFNM.

2.4. Wafer level low frequency noise measurements

Low frequency noise measurements on electron devices are more easily performed on packaged samples rather than at wafer level. There are at least two reasons for this. The first one is the high level of low frequency noise which is generated at the point contacts of the probe tips in the case of wafer level noise measurements [14]. The probe contact noise is mainly $1/f$ noise whose amplitude is proportional to the square of the DC current that crosses the contact and therefore its effect is particularly important in the case of measurements performed with relatively high currents (a few tens of mA) and at very low frequencies ($f < 1$ Hz) as in the case of the electromigration experiments [11]. The second reason which makes wafer level LFNM difficult is the need for an accurate mechanical and electromagnetic shielding of the large volume occupied by the probe station. Probe stations with excellent mechanical stability and high immunity to external interferences may be certainly found on the market, but at a quite high cost. We have recently addressed this specific issue and we have devised a micro probe system dedicated to LFNM on devices available at wafer level. Notwithstanding its low cost, the performances of the system have resulted fully compatible with the requirements for high sensitivity noise measurements [15]. A schematic diagram of the system is reported in Fig. 12. We renounced to the possibility of realizing a probe system capable of hosting an entire 8-inch wafer. The sample holder (7) top plate has a diameter of 3 cm and can therefore host quite large dies. The entire structure is obtained starting from two 4 mm thick aluminum boxes, the cover plates of both being screwed together to form the base (1), which is 14 cm \times 22 cm in size.

One of the boxes is used to form the bottom section (2), which hosts the biasing system and the noise preamplifiers (3) together with the battery pack (4). The other box forms the top cover (5). A ferromagnetic flat base (6) allows the sample holder (7), which has four magnetic disks inserted in its base (8), to slide for a coarse positioning of the DUT. A thin (0.1 mm) PTFE foil (9) allows for electrical insulation. Up to four probes can be hosted onto the base. The probes consist of standard tungsten tips (10) embedded in an insulating holder (11) each of which is mounted on an XYZ precision translator (12). The inner conductor of a RG174 coaxial cable (13) is soldered to a miniature screw wire holder, which is secured to the tungsten tip.

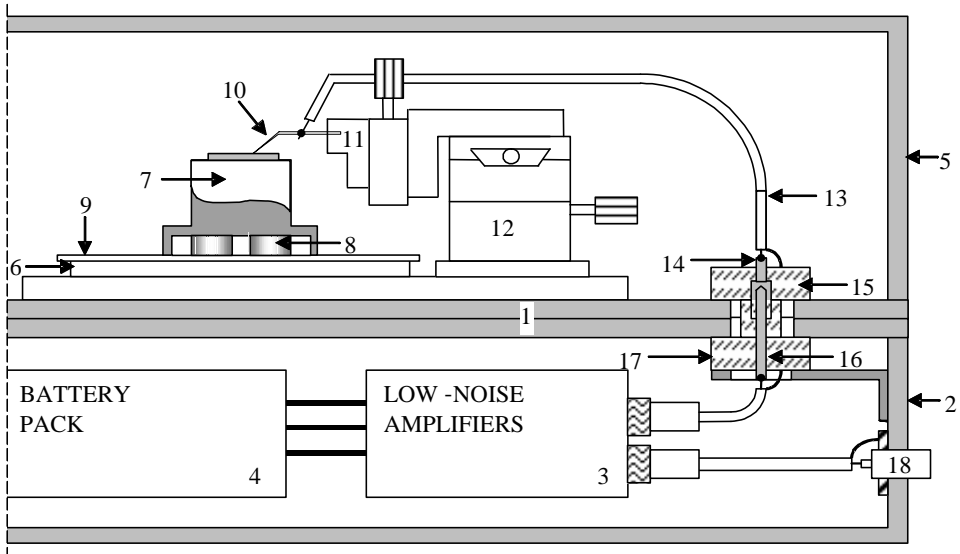


Fig.12. Schematic view of the low noise probe system used for LFNM on wafer level samples.

The other end of the cable is connected to a 4 mm female connector (14), which is inserted in a highly insulating PTFE holder (15). Each female connector has a corresponding male connector (16), which is inserted in a second PTFE holder (17) secured to the bottom section box. Once the base is inserted into the bottom section, electric continuity from the tips to the electronic section is automatically obtained and the electronic section is completely shielded from the environment. At this point one may position the sample holder and contact the DUT pads with the aid of a microscope (not shown in Fig. 12), and put the top cover in place thus obtaining a structure in which the sample is shielded from the electronic section and both are completely shielded from the environment. The results of the measurements of the shot noise of the gate leakage current on a MOS test structure is reported in Fig. 13. Note that the lowest measured shot noise level is as low as $5.65 \text{ fA}/\sqrt{\text{Hz}}$, thus confirming the very high sensitivity that can be obtained with our dedicated probe system.

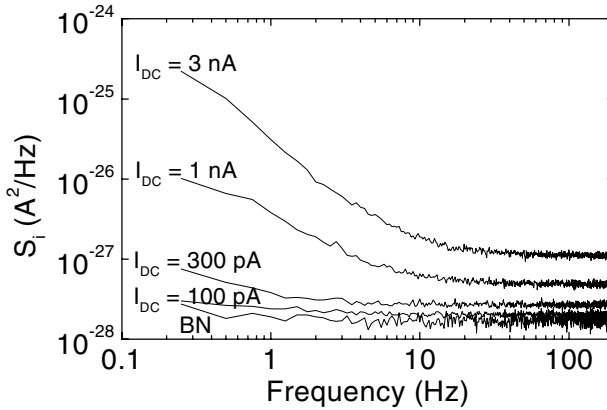


Fig.13. Power spectral density of the current noise measured in a polycrystalline silicon gate MOS structure with a 7 nm thick oxide at different DC current levels. The measurements were performed using the new probe system. The BN of the transresistance amplifier is also shown.

3. Signal Acquisition and Elaboration

Noise spectra estimation in the case of LFNMs is usually performed by means of dynamic signal analyzers. Commercial FFT spectrum analyzers have, however, a few limitations. Usually, only one or two input channels are available thus making the possibility of using LFNMs for performing reliability tests on a large number of samples [12] either impossible or time consuming. Moreover, after performing the calculation of the FFT, the acquired time record is discarded to make room for another one. This fact, when we remember that in order to perform power spectra estimation of down to a few mHz a time record of several thousands of seconds need to be elaborated, not to talk of the case of long term noise measurements [12], leads to a few drawbacks. In the first place, it is seldom possible for an operator to constantly monitor the measurement for detecting possible interferences which may cause spurious increase in the measured spectra. Moreover, one has to make the choice, at the beginning of the measurement, of either privileging frequency resolution at the cost of bandwidth or of privileging bandwidth at the cost of resolution. If one realizes that a different bandwidth-frequency resolution combination was necessary, one has to repeat the measurement with the new parameters. All these problems would be solved if it were possible to store the entire duration of the time record in such a way as to be able to defer the spectral estimation at the conclusion of the measurements. In this way, one could play back the acquired data at a faster speed and make sure that no anomalous behavior occurred during the measurements while selecting the proper combination of bandwidth and frequency resolution. We have in fact designed and realized such a system which, in its early version, is described in [7]. The system we use at present is based on a DSP board that we have purposely developed for LFNMs and uses a PC for controlling the acquisition, storing the data and performing spectral estimation. The system has 8 input channels and the maximum acquisition frequency is 512 Hz, which is largely sufficient for LFNMs. For the connection from the front end and the sampling boards to the PC, we used a fiber optical link in order to avoid the electromagnetic interferences generated by the PC to reach the low noise preamplifiers.

Signal elaboration, either before or after sampling, may be used in order to reach equivalent BN which can be below that of the input preamplifiers. The possibility of performing reliable noise measurements when the noise produced by the DUT is comparable to, or lower than, the BN of the input preamplifier has been demonstrated using different methods [16–18]. We have recently proposed another method for performing reliable very low noise measurements which, although in principle equivalent to the one described in [17], is based on a rather different approach [19]. The circuit configuration of the system is reported in Fig. 14 for the case of voltage noise measurements. The DUT voltage noise V_s is simultaneously amplified by two different channels with identical gains and the two amplified signals are fed to the analog addition and subtraction blocks. The output voltages $x_1(t)$ and $x_2(t)$ can be written as:

$$\begin{cases} x_1(t) = c(t) + u_1(t) \\ x_2(t) = c(t) + u_2(t) \end{cases} \quad (5)$$

where $c(t)$ is due to the input signal and to the EICN of the two amplifiers, $u_1(t)$ is due to the EIVN of the first amplifier and $u_2(t)$ is due to the EIVN of the second amplifier. Therefore, at the output of the addition and subtraction blocks we have:

$$\begin{cases} a(t) = 2c(t) + u_1(t) + u_2(t) \\ s(t) = u_1(t) - u_2(t) \end{cases} \quad (6)$$

At least in the case of LFNM, one can assume that $u_1(t)$, $u_2(t)$ and $c(t)$ are uncorrelated and, therefore, at the output of each channel of the spectrum analyzer in Fig. 14 we have:

$$\begin{cases} S_a(f) = 4S_c(f) + S_{u_1}(f) + S_{u_2}(f) \\ S_s(f) = S_{u_1}(f) + S_{u_2}(f) \end{cases} \quad (7)$$

where $S_x(f)$ is the Power Spectral Density (PSD) of the signal $x(t)$. By subtracting $S_s(f)$ from $S_a(f)$ we obtain an estimate of $S_c(f)$ alone. It is clear that, in the frequency range in which the contribution of the EICN of the amplifiers is negligible, we obtain a direct estimate of the PSD of the noise signal we are interested in. Since the contributions of the EIVN of the amplifiers cancel out, the sensitivity of the measurement method is limited by the contributions of the EICN, whose effect depends on the equivalent impedance of the DUT. This fact implies that in order to measure very low voltage noise, the EICN of the amplifier represents the limiting factor rather than the EIVN. Therefore, using the measurement configuration we propose, one may obtain better noise performances from MOSFET input stage amplifiers (high EIVN and low EICN) rather than from those employing BJTs (low EIVN and high EICN), even in the case of low DUT impedances.

In order to verify the effectiveness of our approach, we used two voltage noise amplifier based on the TLC2201 by Texas Instruments which is characterized by a relatively high EIVN (10 nV/√Hz, $f > 100$ Hz) and by an excellent level of EICN (0.6 fA/√Hz). Two INA141 instrumentation amplifier were used for realizing the adding and subtracting blocks. A resistance R_{10} of 10 Ω was used as DUT. At room temperature the value of the PSD of the voltage fluctuation to be measured is about 407 pV/√Hz. As it can be verified in Fig. 15, the estimation of DUT noise as obtained by using the proposed method is rather good, with an average value of 409 pV/√Hz and a standard deviation of 270 pV/√Hz after 2^{16} averages with a frequency resolution of 25 Hz. It must be noted that the noise produced by the DUT is more than 25 dB below the EIVN of the input. The same method can be used also in the case of current noise measurements [19].

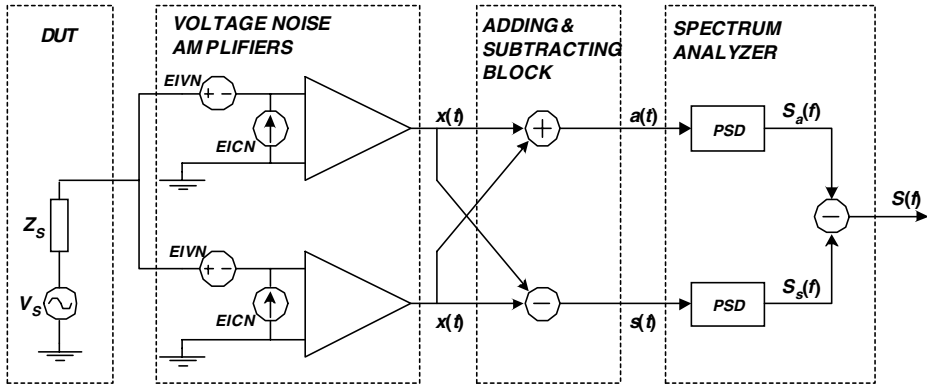


Fig. 14. Block diagram of the new voltage noise measurement system.

Another possible method for reducing the influence of the low frequency noise introduced by the input preamplifiers consists in modulating the bias in the DUT in such a way as to translate the noise to be measured at a frequency where the $1/f$ noise of the amplifier can be neglected. The original noise signal is detected, after amplification, by resorting to synchronous detection schemes [20]. While this method may result effective in a few cases, it must be noted that its application results in a quite complex measurement configuration. It is for this reason that we strongly feel that its use should be avoided whenever possible and that avoiding such complications fully justify the efforts toward the design of very low noise amplifiers for direct coupling to the DUT as those discussed in Sec. 2.2.

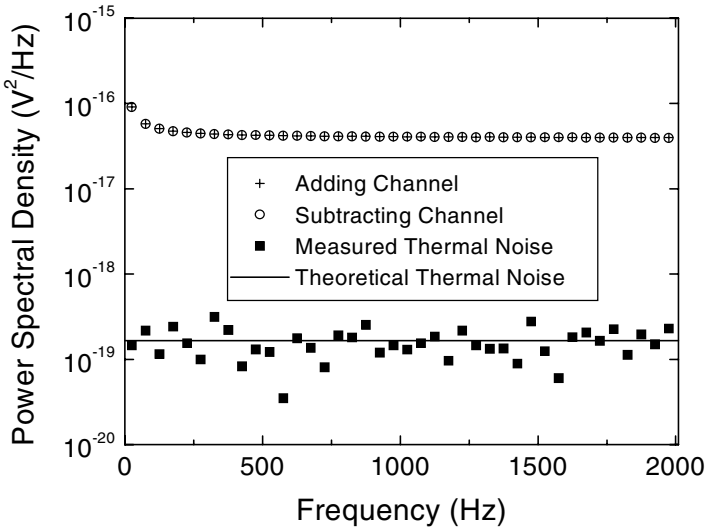


Fig. 15. Power spectra at the output of the adding and subtracting channel and estimated spectrum of the input voltage noise source (a 10Ω resistor).

4. Conclusions

Low frequency noise measurements may represent a powerful tool for the characterization of the quality and reliability of electron devices. The sensitivity which can be obtained by means of this characterization technique may be very high, provided that the BN produced by the instrumentation which is used to build the measurement chain is minimized. Unfortunately, especially in the case in which one is interested in the very low frequency range of the spectrum ($f < 1$ Hz), commercially available instrumentation does not allow to reach sufficient sensitivity for many applications. Therefore one must often resort to purposely designed instrumentation in order to reduce the BN to an acceptable level. In this paper we have reviewed the work done by our research groups in this field over the past few years. In particular we have discussed the design and the performances of very low noise voltage and transresistance amplifiers, of very low noise programmable voltage and current sources, of a high stability thermal chamber, of a dedicated probe systems for LFNM on wafer level devices and of a dedicated multi-channel acquisition system. We have also discussed data elaboration methods for increasing LFNM sensitivity. While in most cases we have obtained excellent results as far as the BN at very low frequencies is concerned, there are still several important issues that need to be addressed, and among them the design of compact size, very low noise, programmable voltage and current sources is one of the most challenging ones.

References

- [1] F. N. Hooge and A. M. Hoppenbrouwers, *If noise in continuous thin gold films*, *Physica* **45** (1969) 386–392.
- [2] J. L. Vossen, *Screening of metal film defects by current noise measurements*, *Appl. Phys. Lett* **23** (1973) 287–289.
- [3] G. Bertotti, M. Celasco, F. Fiorillo and P. Mazzetti, *Thermal equilibrium properties of vacancies in metal through current noise measurements*, *J. Appl. Phys.* **50** (1979) 6948.
- [4] C. Ciofi and B. Neri, *Low-frequency noise measurements as a characterization tool for degradation phenomena in solid-state devices*, *Journal of Physics D* **33** (2000) R199–R216.
- [5] L. Baracchino, G. Basso, C. Ciofi and B. Neri, *Ultralow-noise, programmable, voltage source*, *IEEE Trans. Instr. Meas.* **46** (1997) 1256–1261.
- [6] C. Pace, C. Ciofi and F. Crupi, *Very low noise, high accuracy, programmable voltage reference*, *IEEE Trans. Instr. Meas.* **52** (2003) 1251–1254.
- [7] C. Ciofi, M. De Marinis and B. Neri, *Ultralow-noise PC-based measurement system for the characterization of the metallizations of integrated circuits*, *IEEE Trans. Instr. Meas.* **46** (1997) 798–793.
- [8] C. Ciofi, F. Crupi, C. Pace and G. Scandurra, *Improved trade-off between noise and bandwidth in op-amp based transimpedance amplifier*, Proceedings of IMTC 2004, Como, Italy.
- [9] C. Ciofi, R. Giannetti, V. Dattilo and B. Neri, *Ultra low-noise current sources*, *IEEE Trans. Instr. Meas.* **47** (1998) 78–81.
- [10] C. Ciofi, M. De Marinis and B. Neri, *Wafer level measurement system for SARF characterization of metal lines*, *Microelectron. Reliab.* **36** (1996) 1851–1855.
- [11] B. Neri, C. Ciofi and V. Dattilo, *Noise and fluctuations in submicrometric Al-Si interconnect lines*, *IEEE Trans. Electr. Dev.* **44** (1997) 1454–1459.
- [12] V. Dattilo, B. Neri and C. Ciofi, *Low frequency noise evolution during lifetime tests of lines and vias subjected to electromigration*, *Microelectron. Reliab.* **40** (2000) 1323–1327.
- [13] C. Ciofi, I. Ciofi, S. Di Pascoli and B. Neri, *Temperature controlled oven for low noise measurement systems*, *IEEE Trans. Instr. Meas.* **49** (1999) 546–549.
- [14] A. M. Yassine, T. M. Chen and B. A. Beitman, *Characterization of probe contact noise for probes used in wafer-level testing*, *IEEE Elect. Dev. Lett.* **12** (1991) 200–203.

- [15] C. Ciofi, F. Crupi, C. Pace and G. Scandurra, *Micro-prober for wafer-level low-noise measurements in MOS devices*, *IEEE Trans. Instr. Meas.* **52** (2003) 1533–1536.
- [16] M. Macucci and B. Pellegrini, *Very sensitive measurement method of electron device current noise*, *IEEE Trans. Instrum. Meas.* **40** (1991) 7–12.
- [17] M. Sampietro, L. Fasoli and G. Ferrari, *Spectrum analyzer with noise reduction by cross correlation technique on two channels*, *Rev. Sci. Instrum.* **70** (1999) 2520–2525.
- [18] E. Rubiola and V. Giordano, *A correlation-based noise measurement scheme showing sensitivity below the thermal floor*, Proceedings of International Conference on Noise in Physical Systems and 1/f Fluctuations, Hong Kong (1999) 483–486.
- [19] C. Ciofi, F. Crupi and C. Pace, *A new method for high sensitivity noise measurements*, *IEEE Trans. Instr. Meas.* **51** (2002) 656–659.
- [20] A. M. Yassine and C. T. Chen, *Electromigration noise measurements using a novel AC/DC wafer-level noise measurement system*, *IEEE Trans. Elect. Dev.* **44** (1997) 180–184.